Biomedical Optics EXPRESS

Monitoring the primo vascular system in lymphatic vessels by using window chambers

Jungdae Kim,[1,2] Dong-Hyun Kim,[3] Sharon Jiyoon Jung,[1,4] Hyun-Ji Gil,[1] Seung Zhoo Yoon,[5] Young-Il Kim,[3] and Kwang-Sup Soh[1,*]

[1]*Nano Primo Research Center, Advanced Institute of Convergence Technology, Seoul National University, Suwon 443-270, South Korea*
[2]*Pharmacopuncture Medical Research Center, Korean Pharmacopuncture Institute, Seoul 157-801, South Korea*
[3]*Department of Nano-Optical Engineering, Korea Polytechnic University, Siheung 429-793, South Korea*
[4]*Department of Transdisciplinary Studies, Graduate School of Convergence Science and Technology, Seoul National University, Suwon 443-270, South Korea*
[5]*Department of Anesthesiology, College of Medicine, Korea University, Seoul 02841, South Korea*
[*]*kssoh@phya.snu.ac.kr*

Abstract: This study aims to develop a window chamber system in the skin of rats and to monitor the primo vascular system (PVS) inside the lymphatic vessels along the superficial epigastric vessels. The PVS in lymphatic vessels has been observed through many experiments under *in vivo* conditions, but monitoring the *in vivo* PVS *in situ* inside lymphatic vessels for a long time is difficult. To overcome the obstacles, we adapted the window chamber system for monitoring the PVS and Alcian blue (AB) staining dye solution for the contrast agent. The lymphatic vessels in the skin on the lateral side of the body, connecting the inguinal lymph nodes to the axillary lymph nodes, were the targets for setting the window system. After AB had been injected into the inguinal lymph nodes with a glass capillary, the morphological changes of the stained PVS were monitored through the window system for up to twenty hours, and the changes in the AB intensity in the PVS were quantified by using image processing. The results and histological images are presented in this study.

OCIS codes: (170.0170) Medical optics and biotechnology; (170.0110) Imaging systems; (170.2655) Functional monitoring and imaging; (170.3880) Medical and biological imaging; (170.4580) Optical diagnostics for medicine.

References and links

1. J. C. Sandison, "Observations on the growth of blood vessels as seen in the transparent chamber introduced into the rabbit's ear," Am. J. Anat. **41**(3), 475–496 (1928).
2. Q. Huang, S. Shan, R. D. Braun, J. Lanzen, G. Anyrhambatla, G. Kong, M. Borelli, P. Corry, M. W. Dewhirst, and C. Y. Li, "Noninvasive visualization of tumors in rodent dorsal skin window chambers," Nat. Biotechnol. **17**(10), 1033–1035 (1999).
3. G. M. Palmer, A. N. Fontanella, S. Shan, G. Hanna, G. Zhang, C. L. Fraser, and M. W. Dewhirst, "*In vivo* optical molecular imaging and analysis in mice using dorsal window chamber models applied to hypoxia, vasculature and fluorescent reporters," Nat. Protoc. **6**(9), 1355–1366 (2011).
4. I. Fuhrhop, M. Schroeder, S. L. Rafnsdóttir, L. Viezens, W. Rüther, N. Hansen-Algenstaedt, and C. Schaefer, "Dynamics of microvascular remodelling during tumor growth in bone," J. Orthop. Res. **28**(1), 27–31 (2010).
5. N. M. Biel, J. A. Lee, B. S. Sorg, and D. W. Siemann, "Limitations of the dorsal skinfold window chamber model in evaluating anti-angiogenic therapy during early phase of angiogenesis," Vasc. Cell **6**(1), 17 (2014).
6. D. R. McCormack, A. J. Walsh, W. Sit, C. L. Arteaga, J. Chen, R. S. Cook, and M. C. Skala, "*In vivo* hyperspectral imaging of microvessel response to trastuzumab treatment in breast cancer xenografts," Biomed. Opt. Express **5**(7), 2247–2261 (2014).
7. D. Schaeffer, J. A. Somarelli, G. Hanna, G. M. Palmer, and M. A. Garcia-Blanco, "Cellular migration and invasion uncoupled: increased migration is not an inexorable consequence of epithelial-to-mesenchymal transition," Mol. Cell. Biol. **34**(18), 3486–3499 (2014).
8. E. M. Sevick-Muraca, S. Kwon, and J. C. Rasmussen, "Emerging lymphatic imaging technologies for mouse and man," J. Clin. Invest. **124**(3), 905–914 (2014).
9. M. Weiler, T. Kassis, and J. B. Dixon, "Sensitivity analysis of near-infrared functional lymphatic imaging," J. Biomed. Opt. **17**(6), 066019 (2012).

#255850 Received 15 Dec 2015; revised 28 Jan 2016; accepted 8 Mar 2016; published 14 Mar 2016

10. E. S. Lee, T. S. Kim, and S. K. Kim, "Current status of optical imaging for evaluating lymph nodes and lymphatic system," Korean J. Radiol. **16**(1), 21–31 (2015).
11. S. Kwon and E. M. Sevick-Muraca, "Mouse phenotyping with near-infrared fluorescence lymphatic imaging," Biomed. Opt. Express **2**(6), 1403–1411 (2011).
12. E. R. Clark and E. L. Clark, "Observations on the new growth of lymphatic vessels as seen in transparent chambers introduced into the rabbit's ear," Am. J. Anat. **51**(1), 49–87 (1932).
13. A. Louveau, I. Smirnov, T. J. Keyes, J. D. Eccles, S. J. Rouhani, J. D. Peske, N. C. Derecki, D. Castle, J. W. Mandell, K. S. Lee, T. H. Harris, and J. Kipnis, "Structural and functional features of central nervous system lymphatic vessels," Nature **523**(7560), 337–341 (2015).
14. K. S. Soh, "Bonghan circulatory system as an extension of acupuncture meridians," J. Acupunct. Meridian Stud. **2**(2), 93–106 (2009).
15. M. Stefanov and J. Kim, "Primo vascular system as a new morphofunctional integrated system," J. Acupunct. Meridian Stud. **5**(5), 193–200 (2012).
16. M. Stefanov, M. Potroz, J. Kim, J. Lim, R. Cha, and M. H. Nam, "The primo vascular system as a new anatomical system," J. Acupunct. Meridian Stud. **6**(6), 331–338 (2013).
17. S. J. Lee, S. H. Park, Y. I. Kim, S. Hwang, P. M. Kwon, I. S. Han, and B. S. Kwon, "Adult stem cells from the hyaluronic acid-rich node and duct system differentiate into neuronal cells and repair brain injury," Stem Cells Dev. **23**(23), 2831–2840 (2014).
18. D. J. Cai, J. Chen, Y. Zhuang, M. L. Liu, and F. R. Liang, "Review and comment on the relationship between primo vascular system and meridians," Evid. Based Complement. Alternat. Med. **2013**, 279176 (2013).
19. Y. I. Noh, M. Rho, Y. M. Yoo, S. J. Jung, and S. S. Lee, "Isolation and morphological features of primo vessels in rabbit lymph vessels," J. Acupunct. Meridian Stud. **5**(5), 201–205 (2012).
20. S. H. Lee, K. H. Bae, G. O. Kim, M. H. Nam, Y. B. Choi, H. M. Kwon, Y. Ryu, and K. S. Soh, "Primo vascular system in the lymph vessel from the inguinal to the axillary nodes," Evid. Based Complement. Alternat. Med. **2013**, 472704 (2013).
21. S. J. Jung, K. H. Bae, M. H. Nam, H. M. Kwon, Y. K. Song, and K. S. Soh, "Primo vascular system floating in lymph ducts of rats," J. Acupunct. Meridian Stud. **6**(6), 306–318 (2013).
22. S. J. Jung, S. H. Lee, K. H. Bae, H. M. Kwon, Y. K. Song, and K. S. Soh, "Visualization of the primo vascular system afloat in a lymph duct," J. Acupunct. Meridian Stud. **7**(6), 337–345 (2014).
23. B. H. Kim, "On the kyungrak system," J. Acad. Med. Sci. DPRK. **90**, 1–35 (1963).
24. B. C. Lee, J. S. Yoo, K. Y. Baik, K. W. Kim, and K. S. Soh, "Novel threadlike structures (Bonghan ducts) inside lymphatic vessels of rabbits visualized with a Janus Green B staining method," Anat. Rec. B New Anat. **286**(1), 1–7 (2005).
25. C. Lee, S. K. Seol, B. C. Lee, Y. K. Hong, J. H. Je, and K. S. Soh, "Alcian blue staining method to visualize bonghan threads inside large caliber lymphatic vessels and x-ray microtomography to reveal their microchannels," Lymphat. Res. Biol. **4**(4), 181–190 (2006).
26. H. M. Johng, J. S. Yoo, T. J. Yoon, H. S. Shin, B. C. Lee, C. Lee, J. K. Lee, and K. S. Soh, "Use of magnetic nanoparticles to visualize threadlike structures inside lymphatic vessels of rats," Evid. Based Complement. Alternat. Med. **4**(1), 77–82 (2007).
27. B. C. Lee and K. S. Soh, "Contrast-enhancing optical method to observe a Bonghan duct floating inside a lymph vessel of a rabbit," Lymphology **41**(4), 178–185 (2008).
28. V. Ogay, K. H. Bae, K. W. Kim, and K. S. Soh, "Comparison of the characteristic features of Bonghan ducts, blood and lymphatic capillaries," J. Acupunct. Meridian Stud. **2**(2), 107–117 (2009).
29. I. H. Choi, H. K. Jeong, and Y. K. Hong, " Detection of the primo vessels in the rodent thoracic lymphatic ducts," in *The Primo Vascular System: Its Role in Cancer and Regeneration*, K. S. Soh, K. A. Kang, D. Harrison, eds. (Springer, 2011).

1. Introduction

As bio-imaging methods, optical techniques in *in vivo* experiments have a number of key advantages over other common imaging modalities such as X-ray computed tomography, magnetic resonance imaging, or positron emission tomography. The advantages include high resolution, low cost and an extensive library of contrast agents. A major challenge to bio-imaging in the laboratory is the limited penetration depth imposed by tissue turbidity. The window chamber technique was introduced as a useful tool for avoiding the main limitation due to tissue turbidity [1–3]. This facilitated the study of a wide range of processes such as vascular remodeling [4] and angiogenesis [5], as well as tumor growth [6] and invasion [7]. The window chamber system makes possible various quantitative imaging and analysis techniques for characterizing *in vivo* properties in the field of vascular morphology.

The lymphatics are the most complex and fascinating systems in the body, but also the least understood [8]. In comparison with the blood vasculature, where considerable knowledge has been gained about its structure and function, little is known about the detailed structure of the lymphatic network [9]. The lymphatic vasculature forms a second circulatory system that drains extracellular fluid from tissues and provides an exclusive environment in

#255850 Received 15 Dec 2015; revised 28 Jan 2016; accepted 8 Mar 2016; published 14 Mar 2016

which immune cells can encounter and respond to foreign antigens. Although lymphatics is equally important for the functioning of both the cardiovascular and the immune systems, knowledge of its molecular biology is rudimentary due to the technical difficulties in identifying and isolating lymphatic endothelial cells. Optical imaging techniques have been developed for biomedical imaging of the lymphatic system, and the focus of those techniques has been the visualization of the lymphatic network by using various tracers emitting in the near-infrared spectral ranges [10, 11].The first trial for observations of the new growth of lymphatic vessels was done by introducing a transparent window chamber into a rabbit's ear [12]. A very recent discovery with modern technology showed the existence of lymphatic vessels in the central nervous system [13].

In the last decade, the primo vascular system (PVS) has been actively investigated from the aspects of anatomy [14–16] and cell biology [17]. The PVS was found during a study of the meridian system, which was known to be the conceptional baseline for acupuncture therapy in traditional Eastern medicine. Even though more research to elucidate the relationship between the PVS and acupuncture is still needed [18], the existence of the PVS has been established through numerous anatomical and histological studies. Especially, the presence of the PVS inside lymphatic vessels provides a unique condition for monitoring the dynamic behavior of the PVS in an intact status due to the confinement and the optical transparency of lymphatic vessels.

Several distinctive characteristics of the PVS in lymphatic vessels may be extracted from the accumulation of experimental data until now. Firstly, the average diameter of a typical *in vivo* PVS inside lymph vessels is 53 μm, which is smaller than that of typical lymph vessels (483 μm). To be more specific, a data analysis from a morphological aspect showed that the diameters of the PVS and the lymph vessels near the caudal vena cava of ten rabbits, for example, were 26.0 ± 4.6 μm (mean ± standard deviation (S.D.)) and 258 ± 46 μm, respectively [19]. However, these specific values may depend on the type of animal, the positions of the target lymph vessels, the physiological status, etc [20]. Secondly, the PVS is not attached to the surrounding lymph vessels and freely moves with the liquid flow in the lymph vessels. If the PVS is stained with Alcian blue (AB), a blue threadlike structure may be seen *in vivo* floating inside a transparent lymph duct embedded in fat tissue [21]. Thirdly, a histological study showed that the PVS had rod-shape nuclei. This may easily be confirmed by using 4', 6-diamidino-2-phenylindole (DAPI) staining and observing the stained tissues through a fluorescent microscope [14].

In this study, we focus on monitoring the PVS in lymph vessels near the superficial epigastric vessels of rats by attaching a window chamber system. The conditions for long-term observation require minimal surgery for injecting the staining dye into the lymph nodes and for imaging the PVS inside lymph vessels. Because of the high concentration of hyaluronic acid in the PVS, the most frequently used dye is AB, which stains surface mucopolysaccharides to identify the structure. Compared to the procedures we used for our previous observations of the PVS in deeper areas of the body, such as lumbar vessels and the caudal vena cava, this newly developed procedure with a window will provide a useful method for further study of the dynamic process of the PVS in lymph vessels under more intact conditions.

2. Materials and methods

2.1. Animal preparation

Seven-week-old Sprague-Dawley male rats (weight: 220–280 g) were purchased from DooYeol Laboratory Animal Company (Seoul, Korea) and were housed in a constant temperature-controlled environment (20℃) with 60% relative humidity. All animals were exposed to a 12-hour day and night cycle and allowed free access to water and food. However, on the day before the experiments, the rats were given no food. All procedures involving the animals and their care conformed to the guidelines of the Institutional Animal Care and Use Committee of Woojung BSC, Inc. (Approval number: WJIACUC 20150804-

#255850 Received 15 Dec 2015; revised 28 Jan 2016; accepted 8 Mar 2016; published 14 Mar 2016

03-04), in conjunction with the Advanced Institute of Convergence Technology, Seoul National University, and were in full compliance with current laws and policies.

The rats were anesthetized by intramuscular injection of Zoletil (1.2 mL/kg, Virbac Laboratories, Carros, France) and Xylazine (0.4 mL/kg, Bayer, Korea) in the hind limb. Our target was the lymphatic vessels near the superficial epigastric vessels connecting the inguinal lymph nodes and the axillary lymph nodes. Hair on the lateral side of the rat's body was removed by using a hair clipper and a depilatory (thioglycolic acid 80%, Niclean Cream, Ildong Pharm., Seoul, Korea), as shown in Fig. 1(A). Because the rat's skin is very flexible, we were able to extend the skin and identify the superficial epigastric vessels through the skin with a bright backlight, as shown in the lower panel of Fig. 1(A).

2.2. Window chamber system

The window chamber frame was made of two acrylic plates (25-mm width, 35-mm height, and 2-mm thickness), and a laser cutter was used to remove a 15-mm-square hole from the center, as shown in Fig. 1(B). The four holes in the corners were used to fix the two plates to the skin tissue by using flexible metal wires. The positions of the superficial epigastric vessels were marked on the skin with a bright backlight to position the plates for the window chamber system. After the skin had been removed from the region above the superficial epigastric vessels, we attached the two acrylic plates with folded skin inside them. The window for long-term observation was made of a thin cover glass, which was sealed after the space had been filled with the saline solution.

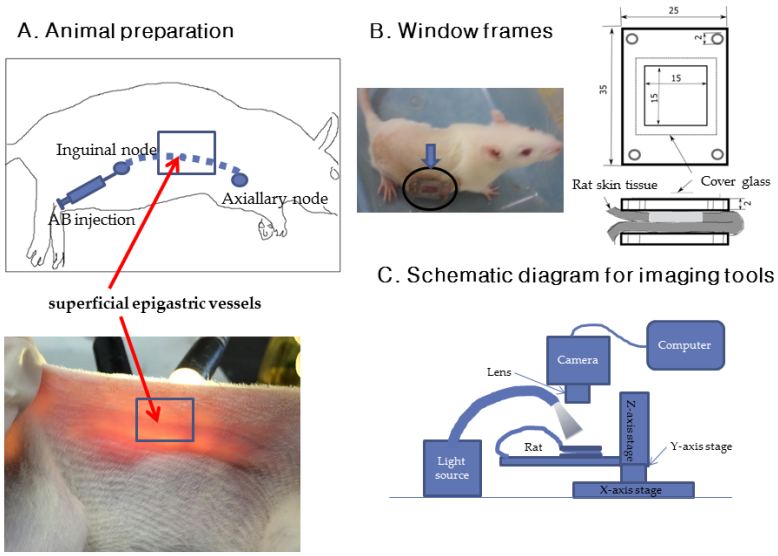

Fig. 1. Experimental procedure for and schematic diagram of the imaging instruments.

2.3. Alcian blue injections and surgeries

Injecting the staining dye into the inguinal node of the rat was tricky and needed careful surgery. Basically, the detailed procedure and the injection tools are presented in [20–22]. In brief, Alcian blue (AB) powder 8GX (Sigma, St. Louis, MO, USA) was dissolved in phosphate-buffered saline (PBS) solution (Life Technology Corp, Waltham, MA, USA) to make the 1% AB staining dye solution (pH 5.5). The solution was stirred by using a vortex machine for 10 seconds and filtered with a 0.22-μm syringe filter (Merck Milli-pore, Darmstadt, Germany). The AB solution was loaded into a 1-mL syringe and kept at a constant

#255850 Received 15 Dec 2015; revised 28 Jan 2016; accepted 8 Mar 2016; published 14 Mar 2016

temperature of 37℃ in a warm bath before use. The original needle tip of the sterile hypodermic syringe was removed and replaced with a luer connector. Thin-walled glass capillaries (World Precision Instruments, Inc., FL, USA; outer and inner diameters of 1.5 and 1.12 mm, respectively) were pulled by using a micropipette puller (PP-830, Narishige Inc., East Meadow, NY, USA) to make a 20-μm tip size on average. The pulled capillary was inserted into the luer connector and was used as an injection needle for the AB dye solution.

The surgeries for the injection and the observation were done at two places on the rat's skin. The first surgery for injection was started by making an incision of the subcutaneous layer of the skin along the linea alba at the navel of a rat lying in the supine position. With further incisions, the skin flap was bent back to expose of the left- or the right-side inguinal lymph nodes. The second surgery for observation was done by making another incision of the subcutaneous layer of the skin just above the superficial epigastric vessel at the corresponding lateral side of a rat lying in a prone position. AB was injected through the glass capillary into the inguinal node until the lymph node had bulged fully; the volume of injected AB was roughly 100 μL with injection speed 50 μL/sec.

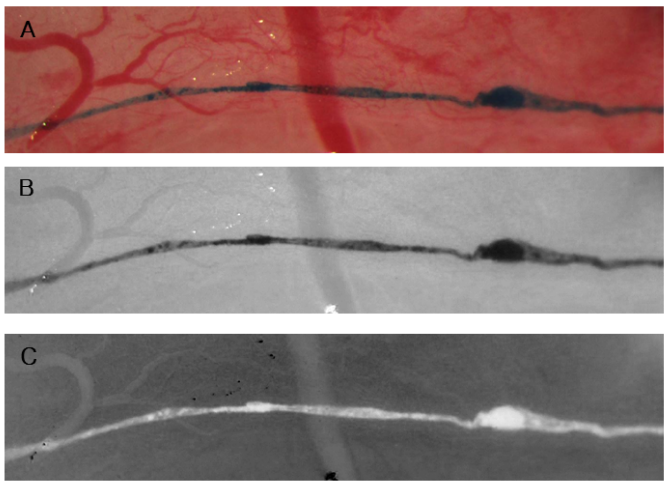

Fig. 2. Imaging process for isolating the intensity of AB-stained tissue in the PVS: (A) the original image, (B) the red component of the original image, and (C) the inverted image of the red component gray image.

2.4. Imaging instruments and imaging process

The monitoring system was composed of basically a microscope with a camera for imaging, a light source for illumination, and motorized linear stages for sample positioning. The images taken by the camera were acquired through a frame grabber and saved in a computer for further analyses. Specifically, the imaging instruments included a stereomicroscope (SZX12, Olympus, Japan) and a light source (100-W metal-halide lamp). The images were taken in the reflective mode above the target area, as shown in Fig. 1(C). For the isolation of the AB-stained region with RGB color images, the software of ImageJ was used to split the RGB 24-bit channels into three 8-bit gray images of Red, Green, and Blue components. We found that among the components, the Red component image dominantly isolated the AB-stained region, as shown in Fig. 2(B). This image was again inverted to make a correlation between the pixel intensity and the concentration of AB solution, as shown in Fig. 2.

#255850 Received 15 Dec 2015; revised 28 Jan 2016; accepted 8 Mar 2016; published 14 Mar 2016

2.5. Histology and confocal imaging

For morphological analysis, some samples were prepared by cutting out the lymphatic vessels, including the primo vessel, in the AB-stained region, and other samples were prepared by extracting the PVS from the lymphatic vessels. For fluorescent staining of the nuclei and the F-actins in the cells, we applied 4',6-diamidino-2-phenylindole (DAPI, D1306, Invitrogen, MO, USA) and phalloidin 488 (A12379, Invitrogen, MO, USA), respectively. The specimens were stained with a 300-nM DAPI solution for 20 minutes and a 6.6-μM phalloidin solution for 30 minutes. After the specimens had been washed, they were covered with mounting solution and were investigated under both a phase contrast & fluorescent microscope (BX51, Olympus, Japan) and a confocal laser scanning microscope (CLSM; C1 plus, Nikon, Japan).

3. Results

3.1. Time-lapse images of the PVS in lymphatic vessels

Immediately after the AB had been injected into the inguinal lymphatic nodes through the glass capillary, a general pattern of the AB flow along the lymphatic vessels was observed within several minutes: The entire inner space of the lymphatic vessel started to fill with the AB solution, and some areas, including the lymphatic valves, were stained more with the blue dye. The distribution of lymphatic vessels and their peristalsis could be clearly observed through the window chamber system. Figure 3 shows a typical time-lapse sequence of images in which the AB-stained patterns inside the lymphatic vessels along the superficial epigastric vessels are seen to change for up to 20 hours after the injection. Usually, the AB-stained threadlike structure was seen inside the lymphatic vessels within one or two hours after injection, and that was the typical observed PVS pattern. In some cases, the AB flow was observed only along the PVS, and no diffusive phenomena were observed in the lymphatic fluid.

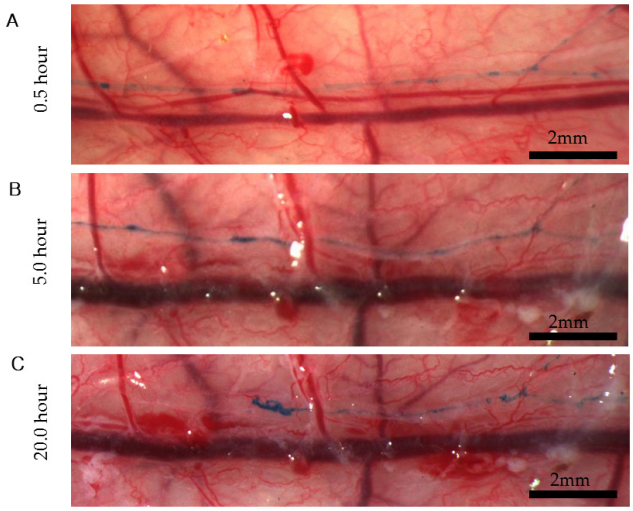

Fig. 3. Time-lapse images after AB had been injected into the inguinal lymph node. The large blood vessels in the figure are superficial epigastric veins. On the left is the caudal vein, and on the right is the cranial wein. The AB flows from left to right. At 20 hours after injection, the SB-stained PVS inside the lymphatic vessel is seen to be disconnected. (Visualization 1 and Visualization 2).

The PVS is freely moving and floating inside the lymphatic vessels, as shown in the supplementary movies. The PVS in the lymphatic vessels seems to have some mechanical

#255850 Received 15 Dec 2015; revised 28 Jan 2016; accepted 8 Mar 2016; published 14 Mar 2016

elasticity, like an extensible string. In this experiment, however, the PVS broke, as can be seen on the left side of Fig. 3(C), after more than one day. This might have been caused by the acidity of AB, which destroys the outer membrane of the PVS, as seen in the electron microscopic images. The morphology of the lymphatic vessels is clearly seen to be different from that of the AB-stained PVS inside them.

3.2. Temporal changes of the AB intensity along the PVS

In order to quantify the temporal changes of the AB concentration in the PVS, we randomly chose two regions for magnified views, and images of those magnified regions were acquired under identical imaging acquisition environments. The changes in the AB intensity were isolated by using the imaging process mentioned in the previous section. To reduce the noise, we used the imaging tool, freehand selection, of the ImageJ to select only regions of interest around the lymphatic vessels in the two regions. The histograms in the right panel of Fig. 4 shows the sum of the pixel intensities in the inverted 8-bit Red component gray images, which corresponds relatively to the AB intensity. The patterns in the two regions are correlated because the regions are in the same lymphatic vessels, but in different areas. The peaks show maximum AB intensities 1 hour after the injection of AB into the regions.

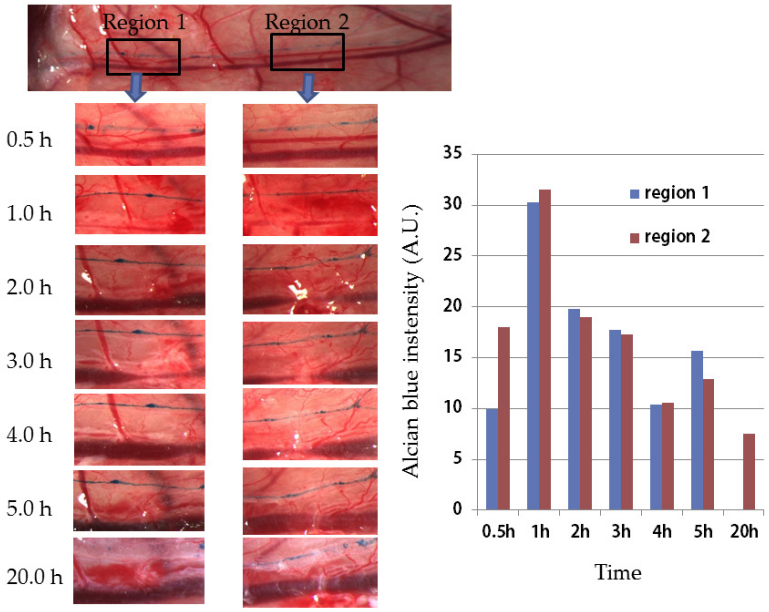

Fig. 4. Temporal changes in the AB intensity along the PVS. Two regions were selected for magnified views, and the images were quantified by image processing the changes in the relative AB intensity for up to 20 hours.

3.3. Histology and confocal images

The cryosectioned sample showed the AB-stained PVS surrounded by the lymphatic wall, as shown in Fig. 5(A). AB stained only the PVS, not the lymphatic wall. The image also shows the PVS inside the lymphatic vessel. A lumen of the PVS can be seen, which implies that the PVS has a flowing channel made of endothelial cells whose nuclei are rod-shaped, as was seen with DAPI staining. The DAPI image in Fig. 5(B) shows many rod-shaped nuclei, a typical characteristic of primo vessels.

#255850 Received 15 Dec 2015; revised 28 Jan 2016; accepted 8 Mar 2016; published 14 Mar 2016

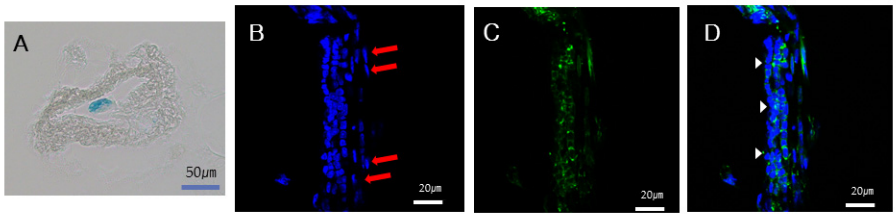

Fig. 5. Histological images and confocal images. (A) A phase contrast image of the AB-stained PVS inside the lymphatic vessel. (B) A DAPI image. The arrows indicate rod-shaped nuclei. The left hand part of the PV shows non-rod-shaped nuclei, which are lymphocytes that aggregated to the PV. (C) A phallodin image showing the cytoskeleton of F-actin. (D) A combined image of B and C. The part belonging to the PV is different from the aggregated lymphocytes (arrow heads).

4. Discussion

The primo vascular system was first reported by Bong-Han Kim in his 1960's work on searching for an anatomical basis for the meridian [23]. He had performed quite extensive and conclusive research through *in vivo* experiments. However, unfortunately, his results could not be reproduced by other scientists because he had not described the materials and the methods he used in detail. One of his main claims was the existence of the PVS inside blood vessels and lymphatic vessels.

A decade ago, a research team at Seoul National University re-initiated PVS research, confirmed the existence of the PVS in various organs, and discovered new characteristics of the PVS [14]. That the PVS was found in adipose tissue and around cancer tissues were important observations. In parallel to these new findings, the team developed new methods for observing and identifying the PVS. The team then performed many studies on the cellular and the material contents inside the PVS, including studies on the functions of the immune cells and the stem cells in the PVS.

During the last ten years, the PVS was confirmed by using various methods with modern technology in many laboratories. Especially, the PVS inside lymph vessels was first observed by injecting the staining dye Janus Green B into the lymph nodes and vessels around the inferior vena cava of rabbits [24]. Staining dyes such as AB [25], fluorescent magnetic nanoparticles [26], methylene blue [27], and other fluorescent agents were used for clearer visualization of the PVS in the lymphatics of experimental animals such as rabbits, rats and mice [28, 29]. As a result, the PVS is known to be a hyaluronic-acid-rich node and duct system within lymphatic and blood vessels, and AB, as used in this work, is to be most effective in displaying the PVS.

The PVS was found to be enriched with small adult stem cells with properties similar to those of very small embryonic-like stem cells. A recent study showed that injection of cells from the PVS partially repaired ischemic brain damage in mice; thus, the PVS may be a pathway for delivering stem cells to regenerate target tissues [17]. Past studies focused mainly on the PVS in the lymph vessels near large blood vessels such as the caudal vena cava, the lumbar vessels, and the thoracic duct. In this experiment, we used a window system to extend the previous work to monitor the long-term behavior of the PVS *in vivo in situ* in the lymph vessels in the skin. Even though the window chamber system allows us to make a long-term monitoring on the PVS, through the current study we found that the PVS is damaged in this experimental condition. Consequently, we need further improvements on experimental factors such as the conditions of anesthesia and the staining dyes to increase the viability of the PVS tissue.

#255850 Received 15 Dec 2015; revised 28 Jan 2016; accepted 8 Mar 2016; published 14 Mar 2016

5. Conclusion

In this study, an imaging system was developed for monitoring the temporal change of the Alcian-blue-stained PVS in lymphatic vessels near the superficial epigastric vessels of rats. The window chamber systems and imaging techniques may provide useful monitoring tools for more systematic research on the dynamic changes of the PVS in the lymphatic system.

Acknowledgments

This research was supported in part by the Basic Science Research Program through the National Research Foundation of Korea (NRF) funded by the Ministry of Science, ICT & Future Planning (grant number: 2013R1A1A2008343 and 2013R1A1A2021577).

#255850 Received 15 Dec 2015; revised 28 Jan 2016; accepted 8 Mar 2016; published 14 Mar 2016